Neurotox Res (2009) 16:416–425
DOI 10.1007/s12640-009-9072-7

Zinc Deficiency Reduces Neurogenesis Accompanied by Neuronal Apoptosis Through Caspase-Dependent and -Independent Signaling Pathways

Hui-Ling Gao · Wei Zheng · Na Xin · Zhi-Hong Chi · Zhen-Yu Wang · Jie Chen · Zhan-You Wang

Received: 25 December 2008 / Revised: 13 April 2009 / Accepted: 13 April 2009 / Published online: 23 June 2009

Abstract Dietary zinc deficiency may affect zinc homeostasis in the brain and lead to reductions of neurogenesis and neuronal survival. However, the mechanisms responsible for the effects of zinc deficiency on hippocampal neurogenesis and neuronal death remain obscure. In the present study, young CD-1 mice were fed with zinc-deficient diet (0.85 ppm) for 5 weeks. The vesicular zinc was reduced at CA1 and CA3 regions of the hippocampus in zinc-deficient mice. The significant decreased zinc ions was associated with a reduction in proliferating cells labeled with bromo-deoxyuridine (BrdU) and immature neurons labeled with doublecortin (DCX) immunoreactivity in the dentate gyrus of the hippocampus. The processes of DCX-positive neurons were shortened, and flexuously went through into the granular cell layer in zinc-deficient hippocampus. There was also a conspicuous increase in the number of TUNEL-positive cells in the hippocampus after zinc-deficient diet treatment. Meanwhile, the apoptosis proteins, including Fas, Fas ligand (FasL), apoptosis inducing factor (AIF), and caspase-3, were significantly activated in zinc-deficient mouse hippocampus. These data suggest that chronic treatment with zinc-deficient diet results in reduction in hippocampal neurogenesis and increases neuronal apoptosis, indicating that zinc deficiency is associated with destroying structural plasticity in the hippocampus.

Keywords Zinc deficiency · Neurogenesis · Apoptosis · Hippocampus

H.-L. Gao · Z.-Y. Wang (✉)
Key Laboratory of Cell Biology, Ministry of Public Health of China, China Medical University, Shenyang 110001, People's Republic of China
e-mail: wangzy@mail.cmu.edu.cn; zhanyouw@hotmail.com

H.-L. Gao · W. Zheng · N. Xin · Z.-H. Chi · Z.-Y. Wang · Z.-Y. Wang
College of Basic Medical Sciences, China Medical University, Shenyang 110001, People's Republic of China

J. Chen
School of Public Health, China Medical University, Shenyang 110001, People's Republic of China

Introduction

The hippocampus is the richest zinc-containing area in the brain (Frederickson et al. 2005). Within the dentate gyrus and CA3 areas, large amounts of chelatable zinc ions exist in the presynaptic vesicles in the giant boutons of mossy fibers. During synaptic activities, these zinc ions are co-released with glutamate to serve as a neuromodulator to modulate different types of receptors, including the amino-3-hydroxy-5-methyl-4-isoxazolepropionic acid (AMPA)/kainate receptor, *N*-methyl-D-aspartate (NMDA) and γ-aminobutyric acid (GABA) receptors, and voltage-gated ion channels (Takeda et al. 2003; Takeda et al. 2004; Smart et al. 2004). Therefore, synaptically released zinc may play an essential role in the induction of long-term potentiation (LTP) in mossy fibers input into CA3 neurons (Li et al. 2001; Takeda et al. 2008a). Recent studies have shown that zinc concentration in the hippocampus is significantly decreased by dietary zinc deficiency (Takeda 2001; Takeda et al. 2008b). Interestingly, epidemiological, clinical, and animal studies have shown that dietary zinc deficiency not only retards the growth status, but also affects several brain functions, including learning and memory defects (Golub et al. 1995; Takeda 2000; Takeda et al. 2008a). However, the underlying mechanism of brain dysfunctions under zinc deficiency is poorly understood.

It has been recognized that hippocampal neurogenesis and neuronal apoptosis are associated with neuronal plasticity. Several studies have correlated changes in hippocampal neurogenesis with altered performance of hippocampus-dependent learning tasks (Aimone et al. 2006; Klempin and Kempermann 2007; Farioli-Vecchioli et al. 2008). The hippocampal dentate gyrus is among the few regions in the brain in which production of new neurons continues in the adulthood. It is well-known that the neuronal progenitor cells in the subgranular zone (SGZ) can differentiate into neurons and glial cells (Prickaerts et al. 2004; Sokolov and Nezlina 2004). Some of the newborn neurons migrate to the granular layer and extend mossy fiber axons, indicating that they are integrated into the functional circuitry of the hippocampus (Gould et al. 1999; Markakis and Gage 1999, van Praag et al. 2002; Joo et al. 2007). Recently, it has been reported that maternal zinc deficiency impaired microtubule-associated protein-2 expression and reduced numbers of nestin-positive stem cells in prenatal and postnatal mouse brain (Wang et al. 2001; Wang et al. 1999). It has also been reported that zinc deficiency impairs neurogenesis by regulating p53-dependent molecular mechanisms (Corniola et al. 2008). Furthermore, several studies have shown that zinc deficiency not only leads to reduction of hippocampal neurogenesis, but also increases neuronal apoptosis (Takeda et al. 2005; Naganska and Matyja 2006; Corniola et al. 2008). Hence, it is reasonable to speculate that changes in dentate neurogenesis and neuronal survival under zinc deficiency may exhibit a close relationship with hippocampal dysfunctions.

To explore the mechanisms responsible for the effects of zinc deficiency on hippocampal neurogenesis and neuronal survival, in the present study, a developmental zinc-deficient mouse model was used, and the proliferation of newborn neurons and the expression of apoptosis-related proteins were analyzed in zinc-deficient mouse hippocampus.

Materials and Methods

Experimental Animals and Zinc-Deficient Diet

CD-1 mice (3-week old, weighing about 13 g) were maintained in stainless steel cages, which were treated by 0.5% EDTA. Mice were randomly assigned to one of the two dietary groups ($n = 60$ in each group), zinc-deficient group and zinc-adequate or control group. Mice were fed 5 weeks with zinc-deficient and zinc-adequate diets, respectively. They were allowed to consume purified, deionized water ad libitum. Zinc contents in the zinc-deficient and zinc-adequate control diets were 0.85 ppm (Egg white-based AIN-76A, Research Diets Company, USA) and 30 ppm, respectively. All experimental procedures were in agreement with the rules of experimental animals at China Medical University, in accordance with the criteria described in the *NIH Guide for the Care and Use of Laboratory Animals*.

Zinc Staining

The *N*-(6-methoxy-8-quinolyl)-*p*-toluenesulfonamide (TSQ) fluorescence staining was performed as described previously (Frederickson et al. 1987; Suh et al. 1999). In brief, mice were killed at the designated time points by decapitation. The brains were removed and frozen in liquid nitrogen, and cryostat sections (20 μm) were prepared. The sections were immersed in a solution of 4.5 μM TSQ (Molecular Probes, Eugene, OR) in 140 mM sodium barbital and 140 mM sodium acetate buffer (pH 10.5) for 1 min. TSQ binding was imaged with a fluorescence microscope. For signal quantification, the mean fluorescence intensity within the hilus of DG, the stratum lucidum of CA3, and the stratum radiatum of CA1 was measured with BZ 8000 analyzes (KEYENCE). Fluorescence intensity was calculated and represented after subtraction of background intensity. Ten sections per animal were averaged to reduce the intra animal variance.

For zinc autometallography (AMG) staining, mice were intraperitoneally injected with sodium selenite (20 mg/kg). One hour after injection, mice were anesthetized and transcardially perfused with saline followed by 3% glutaraldehyde in phosphate buffered saline (PBS, pH 7.4). Brains were removed, postfixed, and cryoprotected. Cryostat sections (10 μm) were prepared, and were placed in jars filled with the AMG developer and incubated for 60 min at 26°C. The AMG development was stopped by replacing the developer with a 5% sodium thiosulphate solution for 10 min (Wang et al. 2003; Chi et al. 2006; Danscher and Stoltenberg 2006; Wang et al. 2006; Zhang et al. 2007; Gao et al. 2008; Zhang et al. 2008; Chi et al. 2009). After mounting, sections were photographed and analyzed with an Olympus microscope equipped with an image analysis system (Motic Images Advanced 3.2). For quantification, 10 sections per animal were checked and the optical density was calculated conventionally (O.D. = ($\log_{10}$ [incident light/transmitted light])).

Administration of 5-Bromo-2-deoxyuridine (BrdU) for Labeling Proliferating Cells in the DG

Seven mice of each group, fed with zinc-deficient and zinc-adequate diets for 5 weeks, respectively, were injected with BrdU (50 mg/kg, i. p., 10 mg/ml in 0.9% NaCl/0.007 N NaOH, B5002, Sigma) 3 times per day (8 h interval) for 2 consecutive days. Mice were transcardially perfused with 4% paraformaldehyde. The brains were dissected and immersed in the same fixative for 3 h at 4°C. Then the samples were cryoprotected overnight in 30% sucrose, and cut into serial sections (30 μm thick, 100 μm intervals) in a cryostat.

For BrdU immunostaining, the following DNA denaturation protocol was followed before immunolabeling to visualize BrdU-labeled nuclei: 2-h incubation in 50% formamide/2× SSC (0.3 M NaCl, 0.03 M sodium citrate) at 65°C, 5-min rinse in 2× SSC, 30-min incubation in 2 N HCl at 37°C, and 10-min rinse in 0.1 M boric acid (pH 8.5). Sections were treated with 0.1 M PBS containing 10% methanol and 3% hydrogen peroxide for 10 min. After rinsing, sections were treated by 5% BSA for 1 h, then incubated overnight at 4°C with the mouse anti-BrdU antibody (1:500, B8434, clone BU-33, Sigma, CA). Sections were washed in PBS, and incubated in the biotinylated rabbit anti-mouse IgG (1:200) for 2 h at RT. After rinsing in 0.05 M TBS, avidin–biotin–peroxidase complex (1:100, ABC Elite Vector) was applied to visualize the reaction sites for 1 h at RT. The sections were immersed in 3,3-diaminobenzidine (DAB) with 0.0033% H_2O_2 for about 10 min. DAB staining was stopped by rinsing with distilled water. The sections were placed on glass slides, dehydrated in alcohol, cleared in xylene, coverslipped with DEPEX, and finally examined with a light microscope.

Doublecortin (DCX) Immunohistochemistry

Free-floating cryostat sections of hippocampus were treated with 0.1 M PBS containing 10% methanol and 3% hydrogen peroxide for 10 min in order to block the endogenous peroxidase. After rinsing with PBS, the sections were treated by 5% bovine serum albumin (BSA) for 1 h, and then incubated overnight with the DCX antibody (1:100; SC-8066, Santa Cruz) at 4°C. The primary antibody was diluted in PBS containing 0.1% BSA and 0.3% Triton X-100. The DCX antibody used in this study is an affinity purified goat polyclonal antibody, which was raised against a peptide mapping at the carboxy terminus of DCX of human origin. Following primary antibody treatment, sections were rinsed in PBS, incubated in the biotinylated rabbit anti-goat IgG (1:200) for 2 h at room temperature (RT). After rinsing in 0.05 M Tris buffered saline (TBS, pH 7.6), the avidin–biotin–peroxidase complex (diluted 1:100, ABC kit, Elite Vector) was applied for 1 h at RT. The following steps were as same as described above.

Control sections were incubated with 5% bovine serum albumin (BSA) instead of the primary antibody. Subsequent incubations were as described above. No positive immunoreaction was found.

Double Immunofluorescence Staining and Confocal Laser Scanning Microscopy

Cryosections were preincubated with normal donkey serum (1:20) for 1 h and then incubated with a mixture of DCX antibody (1:50) and BrdU monoclonal antibody (1:500) overnight at RT. After rinsing, sections were incubated with Texas Red-conjugated donkey anti-goat IgG (1:50) and fluorescein isothiocyanate-conjugated donkey anti-mouse IgG (1:50, Jackson ImmunoResearch Laboratories) for 2 h at RT. Sections were mounted with an anti-fading mounting medium and examined in a confocal laser scanning microscope (SP2, Leica).

Total $BrdU^+$ nuclei, DCX^+ newborn neurons, and $BrdU^+/DCX^+$ double-labeled neurons were counted in the SGZ. The immunostained sections were used to count the numbers of DCX^+ and $BrdU^+$ cells, respectively. The counting of labeled cells was performed using every tenth section, and five sections per mouse were counted. To determine the average number of labeled cells in each mouse, mean values of labeled cells from each section were bilaterally counted, and then the average numbers of labeled cells in each mouse were calculated. The fractions of $BrdU^+$ cells that express DCX were quantified by examination of individual $BrdU^+/DCX^+$ cells in confocal microscopic images. The results were represented as the number of labeled cells per cubic millimeter of the SGZ.

TUNEL Staining

TUNEL staining was performed according to manufacturer's protocol (In Situ Cell Death Detection, POD kit, Roche, Germany). Briefly, cryosections (10 μm) of hippocampus were prepared and incubated in methanol containing 3% H_2O_2 for 10 min. The sections were incubated with the TUNEL reaction mixture, fluorescein-dUTP for 60 min at 37°C. After rinsing, sections were incubated with antifluorescein-POD-conjugate for 30 min at 37°C, and immersed in DAB with 0.0033% H_2O_2 for about 10 min. The sections were washed with distilled water, counterstained with hematoxylin and examined with a light microscope. As a control, the step using the TUNEL reaction mixture was omitted, and nucleotide mixture in reaction buffer was used instead.

To assess TUNEL-positive cell expression, brown grains clustered over hematoxylin stained cells were counted and analyzed in CA1, CA3, and DG regions. Every five brain sections (10 μm thick, 200 μm intervals) were selected from each animal ($n = 5$/group) and processed for TUNEL assay. Data were expressed as number of TUNEL-positive cells/mm^3.

Western Blot Analysis

Nine mice in each group were killed by decapitation. The forebrain, hippocampus, and cerebellum of each mouse were dissected and weighted. The hippocampi were stored at −80°C for Western blot analysis.

For immunoblotting, the hippocampi were homogenized in RIPA buffer containing 50 mM Tris-HCl (pH 7.4), 150 mM NaCl, 1% Nonidet P-40, 1 mM EDTA, 0.25% sodium deoxicolate (DOC), 0.1% SDS, protease inhibitors (1 mM phenylmethylsulfonyl fluoride (PMSF), and 10 mg/ml leupeptin), phosphatase inhibitors (1 mM Na_3VO_4, 1 mM NaF), and incubated at 4°C overnight. The homogenate was centrifuged at 12,000*g* for 30 min and the supernatant was aliquoted and frozen at −80°C.

Total protein extract 30 μg were diluted in an equal volume of electrophoresis buffer (60 mM Tris-HCl, pH 6.8, 25% glycerol, 2% SDS, 14.4 M β-mercaptoethanol, 100 mg/ml bromophenol blue) and boiled for 5 min. Proteins were separated by 10% SDS-polyacrylamide gels (for resolution 16–68 kDa protein) and blotted to polyvinylidene difluoride (PVDF) membranes (Millipore, CA) in a wet electron transfer device (45 V, 15 h). The membranes were incubated with 5% defatted milk for 3 h at RT. Then they were incubated with the following primary antibodies: goat polyclonal anti-DCX antibody (1:1000), goat polyclonal anti-apoptosis inducing factor (AIF, 1:500, Santa Cruz), rabbit polyclonal anti-caspase-3 (1:500, BD), rabbit polyclonal anti-Fas (1:500, Santa Cruz), rabbit polyclonal anti-FasL (1:500, Santa Cruz), and mouse monoclonal anti-GAPDH (1:10000, KC-5G5, Kang Chen, CA), respectively, overnight at 4°C. After three washes in TBS/Tween-20, the membranes were incubated in HRP-conjugated rabbit anti-goat antibody (1:5000), or HRP-conjugated goat anti-rabbit antibody (1:5000) or HRP-conjugated goat anti-mouse antibody (1:5000) for 2 h at RT. Following two washes in TBS/Tween-20, immunolabeled protein bands were detected using an enhanced chemiluminescence (ECL) kit (Pierce, CA) and were visualized by exposure to Kodak-XAR film. After development, the band intensities were quantified using an Image-pro Plus 6.0 analysis software.

Data Analysis

All statistical analyses were carried out using a program SPSS 13.0. All values were represented as mean ± standard deviation (SD). Comparisons were made using Student's *t*-test. $P < 0.05$ was considered significant.

Results

Dietary Zinc Deficiency Causes Poor Growth and Low Hippocampal Zinc Loading in Developing Mouse

Low dietary zinc status may cause poor growth in animals (Takeda et al. 2001), we therefore monitored the body weight gain of zinc-deficient mice and controls. As shown in Fig. 1a, zinc-deficient mice grew slower than controls. The body weight of zinc-deficient mice (17.51 ± 3.98 g) was significantly lower than that of control mice (31.97 ± 3.66 g) over a period of 5 weeks (Fig. 1b). Furthermore, zinc deficiency also caused a lower weight of different brain regions, including the forebrain, the cerebellum, and the hippocampus (Fig. 1c).

To evaluate the chelatable zinc accumulation in hippocampal mossy fibers, we employed both TSQ fluorescence and AMG staining on hippocampal sections. Both approaches showed that zinc ions were located in mossy fibers from DG to CA3 area (Fig. 1d, e, g, h). In the DG, TSQ fluorescence was not different between zinc deficiency group and control group. However, the intensity of fluorescence in the CA1 and CA3 area of zinc-deficient mice was weaker than that of control mice (Fig. 1f). The similar results were also detected in the AMG staining of the hippocampus (Fig. 1g, h). The density of AMG staining was decreased obviously in the CA1 and CA3 region of the zinc deficiency group (Fig. 1i).

Decreased DCX^+, $BrdU^+$, and $BrdU^+/DCX^+$ Cells in the Hippocampus of Zinc-Deficient Mice

To investigate whether hippocampal neurogenesis is impaired by zinc deficiency, the distribution and expression of DCX, a marker for newborn neurons, were analyzed by immunohistochemistry and Western blot. Immunostaining revealed that DCX^+ cells were predominately located in the SGZ (Fig. 2a–d). DCX^+ cells had either a round or fusiform cell body with long processes extending to the granular cell layer (Fig. 2a–d). In zinc-deficient mice, the processes of DCX^+ cell were shortened and their branches were reduced (Fig. 2c, d). Cell counting analysis demonstrated that the number of total DCX^+ cells in zinc deficiency group was obviously less than that in the control group ($P < 0.01$) (Fig. 2e). Western blot results showed that DCX protein was detectable in 8-week-old mouse hippocampus as a 40-kDa-immunostained polypeptide (Fig. 2f). In comparison with zinc-deficient mice to controls, densitometry of DCX immunoreactive bands showed that hippocampal DCX levels in the zinc-deficient mice were substantially lower than that in control mice ($P < 0.01$, Fig. 2f).

We further analyzed the hippocampal neurogenesis by measuring BrdU-immunoreactivity in the hippocampus. Consistent with DCX immunostaining, $BrdU^+$ nuclei, which represent proliferating cells, were also located in the SGZ (Fig. 2g–j). The average number of $BrdU^+$ nuclei in the SGZ in zinc-deficient mice was less than that in controls ($P < 0.05$, Fig. 2k). Confocal microscopic results showed that the number of double-labeled $BrdU^+/DCX^+$ neurons were lower in zinc deficiency group than that in

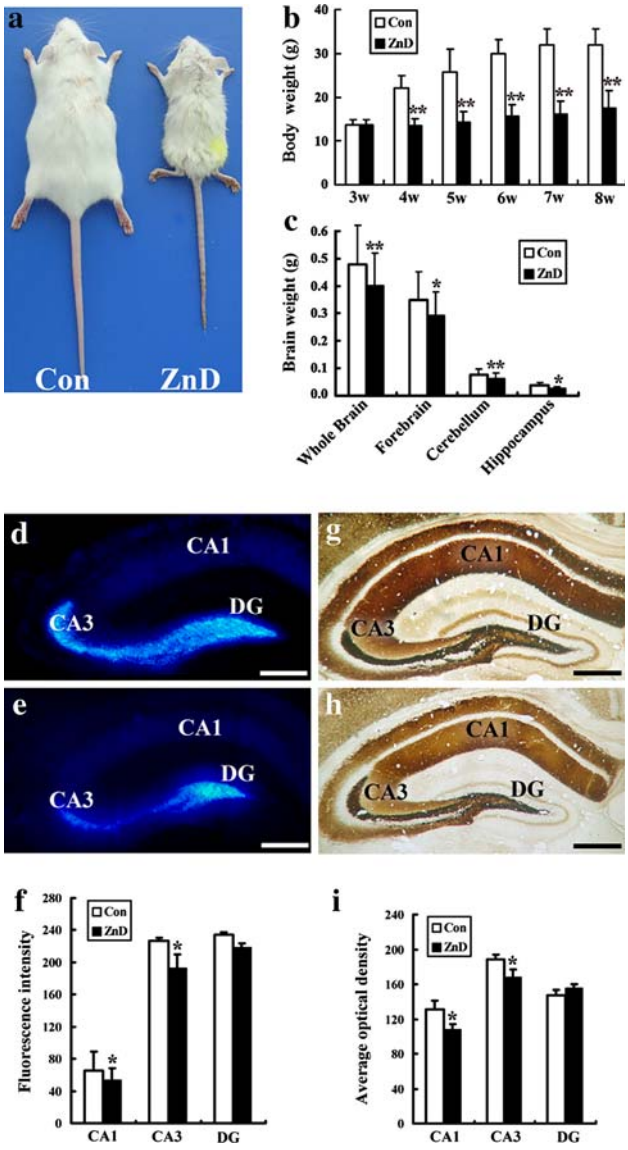

Fig. 1 Reduced body and brain weight and hippocampal vesicular zinc accumulation in zinc-deficient mice. Three-week-old mice were fed with a control or zinc-deficient diet for 5 weeks. **a** Gross appearance of a control (Con) and a zinc-deficient mouse (ZnD) at 8 weeks of age. **b** From the 2nd to 5th week fed with zinc-deficient diet, body weights of zinc-deficient mice were significantly decreased ($n = 30$). **c** At 8 weeks of age, the weights of whole brain, forebrain, cerebellum, and hippocampus were all decreased in zinc deficiency group ($n = 9$). **d–f** TSQ staining showing that vesicular zinc concentration in CA1 and CA3 areas in zinc deficiency group **e** was lower than that in control (**d**, $n = 5$). **g–i** AMG staining showing that vesicular zinc concentration in CA1 and CA3 regions of the zinc deficiency group **h** was decreased significantly compared with control (**g**, $n = 5$). *CA1* CA1 area of hippocampus; *CA3* CA3 area of hippocampus; *DG* dentate gyrus. * $P < 0.05$, ** $P < 0.01$. Bars = 20 μm

control group ($P < 0.05$, Fig. 3). These results indicate that hippocampal neurogenesis is markedly reduced during zinc deficiency.

Zinc Deficiency Results in an Increase in Hippocampal Neuronal Death Through Fas/FasL and AIF Pathways

To examine whether zinc deficiency results in hippocampal neuronal death, the peroxidase TUNEL staining was performed on hippocampal sections from both zinc-deficient and control mice. In control hippocampus, few TUNEL-positive neurons could be observed (Fig. 4a–c). However, in zinc deficiency group, the number of TUNEL-stained cells was elevated in all analyzed regions (CA1, CA3, and DG) of the hippocampus (Fig. 4d–f). Quantitative results indicated that the number of TUNEL-positive cells in zinc-deficient hippocampus was significantly increased in the subareas (CA1, CA3, and DG) of the hippocampus ($P < 0.01$, Fig. 4g). These results suggest that dietary zinc deficiency may cause hippocampal neuronal death.

We next examined whether Fas/FasL, caspase-3, and AIF are involved in zinc deficiency-induced hippocampal cell apoptosis with Western blot immunoassays. It is well-known that Fas/FasL and AIF are pro-apoptotic molecules related to neuronal cell apoptosis (Didier et al. 2004; Strosznajder and Gajkowska 2006). Caspase-3 is one of the key executioners in several apoptotic pathways and is a cytosolic protein as an inactive proenzyme. It is activated by proteolytic cleavage into the 20 and 11 kDa active subunits. As shown in Fig. 5, all checked proteins were detected in bands located at 35 kDa for Fas, 37 kDa for FasL, 66 kDa for AIF, 32 kDa for procaspase-3, and 20 kDa for cleaved caspase-3. Following *t*-test analyses, statistically significant increases in expression levels of Fas and FasL were detected in zinc-deficient hippocampus ($P < 0.05$, Fig. 5a). The cleaved caspase-3 (active) was also increased evidently, but not the procaspase-3 (inactive), in zinc deficiency mice (Fig. 5b). On the other hand, zinc deficiency enhanced the expression of AIF, a caspase-independent apoptotic molecule ($P < 0.05$, Fig. 5c). Thus, these results indicate that dietary zinc deficiency-induced hippocampal cell death may be through several apoptosis signaling pathways.

Discussion

The hippocampus is the most responsive area in the brain to dietary zinc deficiency (Takeda et al. 2001). It has been reported that adult rats show significant learning and memory deficits if their mothers are mildly or severely zinc deficient during late pregnancy and lactation (Halas et al. 1986; Halas et al. 1983; Wang et al. 2001). Dietary zinc deficiency results in the impairment of LTP at the mossy fibers to CA3 synapses (Lu et al. 2000; Takeda et al. 2008b). Using zinc specific TSQ and AMG techniques, in the present study, we showed that zinc concentration was

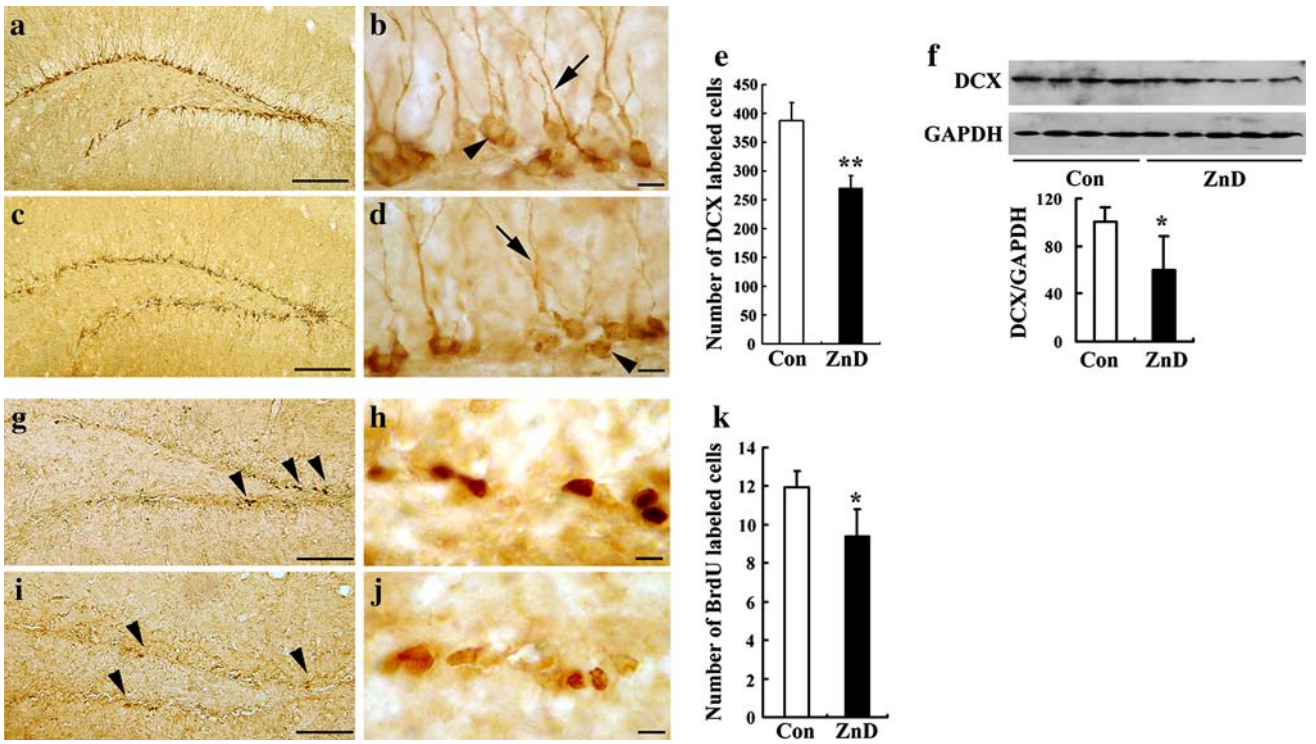

Fig. 2 Decreased hippocampal immature neuronal population and proliferation in zinc-deficient mice. **a**–**d** DCX immunohistochemistry showing the morphology of newly born neurons in the hippocampal dentate gyrus of control (**a**, **b**) and zinc-deficient mouse (**c**, **d**). In control group, DCX^+ cells were located in the SGZ, with round or fusiform cell bodies (*arrowheads*) and long processes (*arrows*) crossing into the granular cell layer (**a**, **b**). In zinc deficiency group, DCX^+ cell bodies (*arrowheads*) were smaller and weakly stained (**c**, **d**). Moreover, DCX^+ processes (*arrows*) were shortened and their branches were decreased obviously (**c**, **d**). **e** Quantitative analysis showing that the number of total DCX^+ cells in SGZ in zinc deficiency group was significantly decreased than that in control group. **f** Western blot showing a reduction of DCX expression in hippocampus of zinc deficiency group compared to control ($n = 9$). GAPDH was used as a loading control. **g**–**j** BrdU immunostaining showing the distribution of $BrdU^+$ nuclei (*arrowheads*) in the SGZ in control group (**g**, **h**) and zinc deficiency group (**i**, **j**). **k** $BrdU^+$ nuclei counts were graphically quantified. The number of $BrdU^+$ nuclei in zinc deficiency group was less than that in control group ($n = 7$). * $P < 0.05$, ** $P < 0.01$. Scale bars = 50 μm (**a**, **c**, **g**, **i**), 10 μm (**b**, **d**, **h**, **j**)

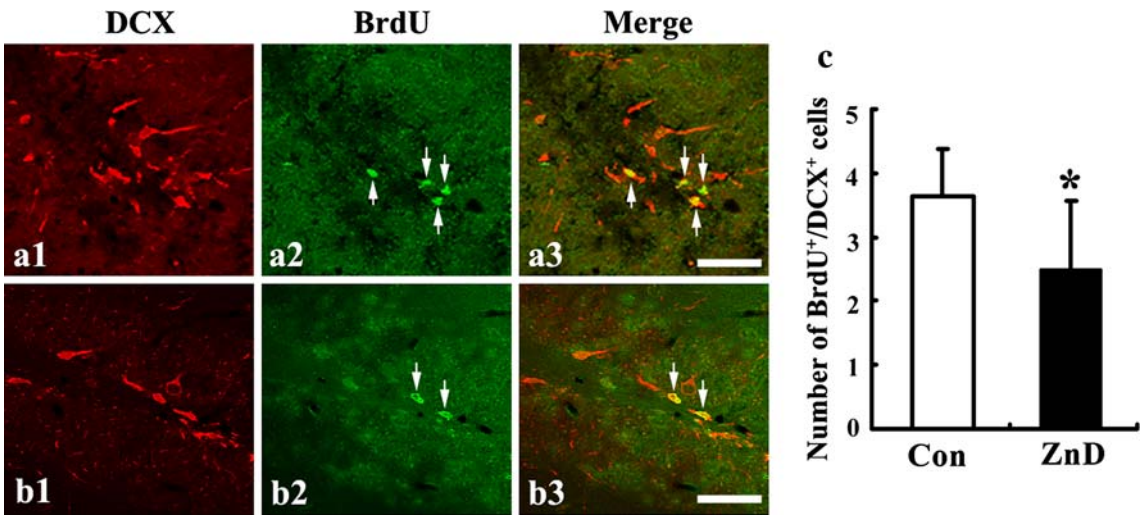

Fig. 3 Confocal images showing the distribution of newly born neurons double labeled with DCX (**a1**, **b1**) and BrdU (**a2**, **b2**) in the SGZ in control (**a1**–**a3**) and zinc-deficient group (**b1**–**b3**). *Arrows* indicate $BrdU^+$ nuclei colocalized with DCX. **c** The reduction of newly born neurons ($DCX^+/BrdU^+$) in zinc-deficient group was graphically quantified ($n = 7$). * $P < 0.05$. Scale bars = 20 μm

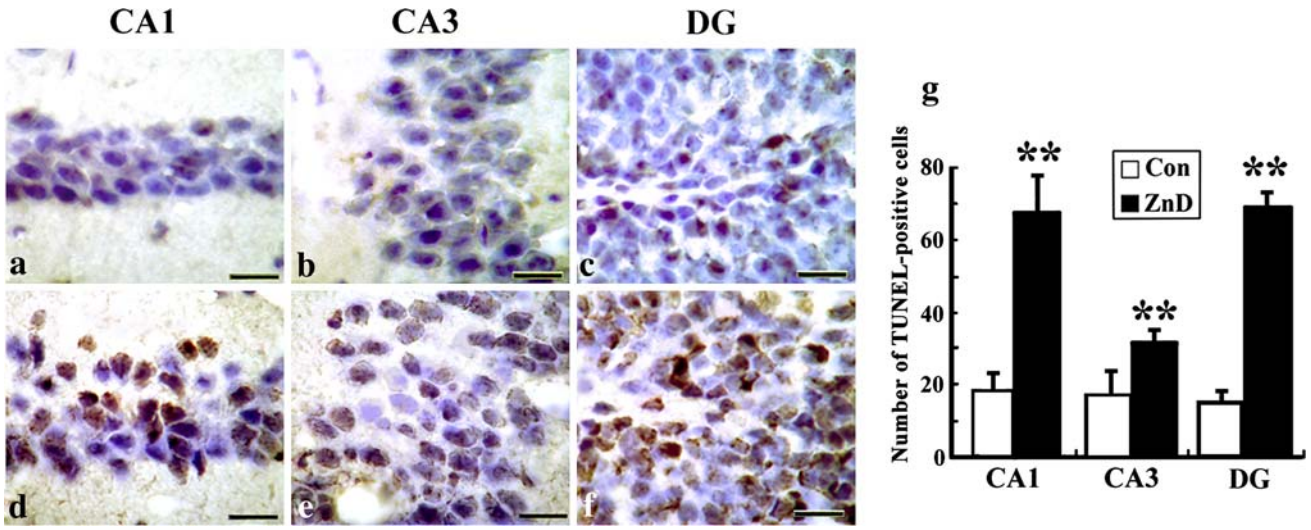

Fig. 4 Zinc deficiency increases neuronal cell death in hippocampal CA1, CA3, and DG. **a–c** In control group, few cells were TUNEL positive in the pyramidal cell layer of CA1 and CA3 regions and the granular cell layer of DG. **d–f** In zinc deficiency group, TUNEL-positive apoptotic cells in CA1, CA3, and DG were increased obviously. **g** Quantitative analysis showing that the number of TUNEL-positive cells was markedly elevated in CA1, CA3, and DG in zinc deficiency group ($n = 7$). ** $P < 0.01$. Scale bars = 20 μm

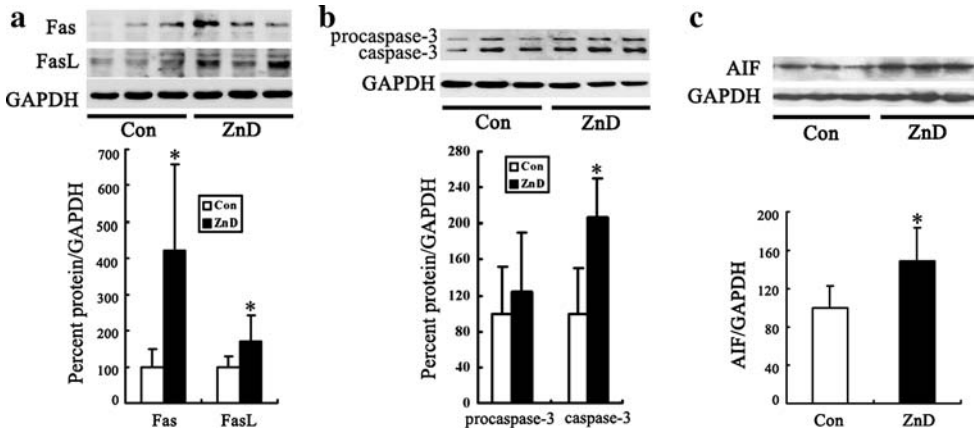

Fig. 5 Expression levels of apoptosis proteins in the hippocampus. Representative images of immunoblots were shown with antibodies against Fas, FasL, caspase-3, and AIF, respectively. GAPDH was used as a loading control. **a** Expression levels of both Fas and FasL proteins were increased in zinc deficiency group. **b** Zinc deficiency increased the level of cleaved caspase-3. In contrast, there was no obvious difference in procaspase-3 between groups. **c** The level of AIF, a caspase-independent apoptosis protein, was elevated in zinc deficiency group. * $P < 0.05$ ($n = 9$)

diminished in hippocampal CA1 and CA3 regions in the zinc-deficient mice. This supports the notion that the decrease of hippocampal vesicular zinc may be critical for transient learning impairment under dietary zinc deficiency (Takeda et al. 2000). Most importantly, the mechanisms underlying the effects of zinc deficiency on hippocampal neurogenesis and neuronal apoptosis have been analyzed in the present study.

Zinc deficiency-induced decrease in granule cell neurogenesis observed in our study is likely to have detrimental effects on neuronal circuits in the hippocampus at both structural and functional levels. New neurons are born within the dentate SGZ throughout life, and are capable of migrating into the granule cell layer (Kuhn et al. 1996). Several studies have shown that hippocampal neurogenesis may be involved in specific types of hippocampal-dependent learning and memory (Shors et al. 2001; Shors et al. 2002; Santarelli et al. 2003; Saxe et al. 2006; Winocur et al. 2006). A reduction in the number of newly born granule cells may influence mossy fiber innervations of the CA3 region, altering neuronal connectivity, pyramidal cell excitability, and memory formation (Treves and Rolls 1994; Kempermann et al. 2004; Kesner and Rogers 2004). In the present study, we showed that dietary zinc deficiency resulted in a reduction in proliferating cells (labeled with BrdU) and newborn neurons (labeled with DCX), and

impaired the newborn granule cell morphology. It is known that dendrites play an essential role in neuronal signaling (Barinaga 1995), and aberrations in dendritic morphology may alter their functional characteristics (Kaech et al. 1996; Bywood and Johnson 2000). The size of cell bodies and the complexity of the dendritic tree in maturing granule cells have been shown to correlate with changes in their electrophysiological properties (Liu et al. 2000; Ambrogini et al. 2004a, b). In this respect, zinc deficiency-induced changes in dendritic morphology of DCX-positive neurons might be associated with brain dysfunctions.

Our observation shows that zinc deficiency induced a drastic raise in the number of TUNEL-positive cells in hippocampus is consistent with previous works showing increase in hippocampal neuronal death under dietary zinc deficiency (Takeda et al. 2005). With zinc chelator TPEN-induced zinc-deficient cell models, previous studies have shown that zinc deficiency induces oxidative DNA damage and apoptosis via p53-mediated and caspase-dependent mechanisms (Takeda et al. 2005). With our mouse model, we showed that expression levels of cleaved caspase-3 as well as Fas and FasL were increased in zinc-deficient hippocampus. It is well-known that FasL is a death ligand and can directly induce apoptosis through binding to its receptor, Fas, and activating caspase cascades (Didier et al. 2004; Guan et al. 2006; Strosznajder and Gajkowska 2006). And caspase-3 is key molecule in several apoptotic pathways and is a cytosolic protein as an inactive proenzyme. Thus, our data suggest that the zinc deficiency-induced hippocampal neuronal death is probably regulated via the Fas/FasL/caspase signaling pathway. On the other hand, the expression level of AIF was also increased in zinc-deficient hippocampus, suggesting that zinc deficiency induces caspase-independent apoptosis that is associated to the nuclear translocation of the mitochondrial AIF. Hence, it is likely that both caspase-dependent and -independent pathways are involved in zinc deficiency-induced neuronal loss in mouse hippocampus.

It has been reported that neuronal apoptosis appears to be related to changes in neurogenesis to some extent in several brain injury models such as seizure and trauma (Jessberger et al. 2005; Rola et al. 2006). In these cases, increase in both apoptotic neurons and newborn neurons are coexisted in hippocampus, suggesting that neuronal apoptosis induces neurogenesis, which is considered as a protective response to compensate the neuronal loss caused by seizure and brain trauma. In contrast, our data indicate that dietary zinc deficiency results in reductions in both proliferating/newborn neurons and neuronal survival. This is consistent with a recent work showing that zinc deficiency impairs neurogenesis accompanied by increase in numbers of TUNEL-positive neurons in hippocampus (Corniola et al. 2008). These suggest that zinc deficiency appears to be unique for the relationship between hippocampal neurogenesis and apoptosis. Because of different mechanisms and labeling conditions for newborn neurons and apoptotic cells, there is no direct comparison between the newborn and apoptotic cells at the same time. Nevertheless, our results showed that the increased apoptotic neurons along with the decreased newborn neurons were coexisted in zinc-deficient hippocampus, indicating that zinc deficiency is associated with destroying structural plasticity in the hippocampus. However, whether newborn neurons undergo apoptosis in zinc-deficient brain remains to be examined.

Acknowledgments The study was supported by the Natural Science Foundation of China (30370452, 30770680), the Program for New Century Excellent Talents in University (NCET-04-0288), the China Postdoctoral Science Foundation (2005037008), and the Specialized Research Fund for the Doctoral Program of Higher Education (SRFDP-20060159001).

References

Aimone JB, Wiles J, Gage FH (2006) Potential role for adult neurogenesis in the encoding of time in new memories. Nat Neurosci 9:723–727

Ambrogini P, Lattanzi D, Ciuffoli S, Agostini D, Bertini L, Stocchi V, Santi S, Cuppini R (2004a) Morpho-functional characterization of neuronal cells at different stages of maturation in granule cell layer of adult rat dentate gyrus. Brain Res 1017:21–31

Ambrogini P, Orsini L, Mancini C, Ferri P, Ciaroni S, Cuppini R (2004b) Learning may reduce neurogenesis in adult rat dentate gyrus. Neurosci Lett 359:13–16

Barinaga M (1995) Dendrites shed their dull image. Science 268: 200–201

Bywood PT, Johnson SM (2000) Dendrite loss is a characteristic early indicator of toxin-induced neurodegeneration in rat midbrain slices. Exp Neurol 161:306–316

Chi ZH, Wang X, Wang ZY, Gao HL, Dahlstrom A, Huang L (2006) Zinc transporter 7 is located in the cis-Golgi apparatus of mouse choroid epithelial cells. Neuroreport 17:1807–1811

Chi ZH, Feng WY, Gao HL, Zheng W, Huang L, Wang ZY (2009) ZNT7 and Zn2+ are present in different cell populations in the mouse testis. Histol Histopathol 24:25–30

Corniola RS, Tassabehji NM, Hare J, Sharma G, Levenson CW (2008) Zinc deficiency impairs neuronal precursor cell proliferation and induces apoptosis via p53-mediated mechanisms. Brain Res 1237:52–61

Danscher G, Stoltenberg M (2006) Silver enhancement of quantum dots resulting from (1) metabolism of toxic metals in animals and humans, (2) in vivo, in vitro and immersion created zinc-sulphur/zinc-selenium nanocrystals, (3) metal ions liberated from metal implants and particles. Prog Histochem Cytochem 41:57–139

Didier A, Windisch W, Pfaffl MW (2004) Elevated caspase-3 and Fas mRNA expression in jejunum of adult rats during subclinical zinc deficiency. J Trace Elem Med Biol 18:41–45

Farioli-Vecchioli S, Saraulli D, Costanzi M et al (2008) The timing of differentiation of adult hippocampal neurons is crucial for spatial memory. PLoS Biol 6:e246

Frederickson CJ, Kasarskis EJ, Ringo D, Frederickson RE (1987) A quinoline fluorescence method for visualizing and assaying the

histochemically reactive zinc (bouton zinc) in the brain. J Neurosci Methods 20:91–103
Frederickson CJ, Koh JY, Bush AI (2005) The neurobiology of zinc in health and disease. Nat Rev Neurosci 6:449–462
Gao HL, Xu H, Wang X, Dahlstrom A, Huang L, Wang ZY (2008) Expression of zinc transporter ZnT7 in mouse superior cervical ganglion. Auton Neurosci 140:59–65
Golub MS, Keen CL, Gershwin ME, Hendrickx AG (1995) Developmental zinc deficiency and behavior. J Nutr 125:2263S–2271S
Gould E, Tanapat P, Hastings NB, Shors TJ (1999) Neurogenesis in adulthood: a possible role in learning. Trends Cogn Sci 3: 186–192
Guan QH, Pei DS, Zong YY, Xu TL, Zhang GY (2006) Neuroprotection against ischemic brain injury by a small peptide inhibitor of c-Jun N-terminal kinase (JNK) via nuclear and non-nuclear pathways. Neuroscience 139:609–627
Halas ES, Eberhardt MJ, Diers MA, Sandstead HH (1983) Learning and memory impairment in adult rats due to severe zinc deficiency during lactation. Physiol Behav 30:371–381
Halas ES, Hunt CD, Eberhardt MJ (1986) Learning and memory disabilities in young adult rats from mildly zinc deficient dams. Physiol Behav 37:451–458
Jessberger S, Romer B, Babu H, Kempermann G (2005) Seizures induce proliferation and dispersion of doublecortin-positive hippocampal progenitor cells. Exp Neurol 196:342–351
Joo JY, Kim BW, Lee JS, Park JY, Kim S, Yun YJ, Lee SH, Rhim H, Son H (2007) Activation of NMDA receptors increases proliferation and differentiation of hippocampal neural progenitor cells. J Cell Sci 120:1358–1370
Kaech S, Kim JB, Cariola M, Ralston E (1996) Improved lipid-mediated gene transfer into primary cultures of hippocampal neurons. Brain Res Mol Brain Res 35:344–348
Kempermann G, Wiskott L, Gage FH (2004) Functional significance of adult neurogenesis. Curr Opin Neurobiol 14:186–191
Kesner RP, Rogers J (2004) An analysis of independence and interactions of brain substrates that subserve multiple attributes, memory systems, and underlying processes. Neurobiol Learn Mem 82:199–215
Klempin F, Kempermann G (2007) Adult hippocampal neurogenesis and aging. Eur Arch Psychiatry Clin Neurosci 257:271–280
Kuhn HG, Dickinson-Anson H, Gage FH (1996) Neurogenesis in the dentate gyrus of the adult rat: age-related decrease of neuronal progenitor proliferation. J Neurosci 16:2027–2033
Li Y, Hough CJ, Frederickson CJ, Sarvey JM (2001) Induction of mossy fiber → CA3 long-term potentiation requires translocation of synaptically released Zn2+. J Neurosci 21:8015–8025
Liu Y, Bao J, Lai H, Yang C, Feng X, Li J (2000) Structural changes of neurons in hippocampus from infantile rats exposed to hyperbaric oxygen. Chin J Traumatol 3:206–209
Lu YM, Taverna FA, Tu R, Ackerley CA, Wang YT, Roder J (2000) Endogenous Zn(2+) is required for the induction of long-term potentiation at rat hippocampal mossy fiber-CA3 synapses. Synapse 38:187–197
Markakis EA, Gage FH (1999) Adult-generated neurons in the dentate gyrus send axonal projections to field CA3 and are surrounded by synaptic vesicles. J Comp Neurol 406:449–460
Naganska E, Matyja E (2006) Apoptotic neuronal changes enhanced by zinc chelator—TPEN in organotypic rat hippocampal cultures exposed to anoxia. Folia Neuropathol 44:125–132
Prickaerts J, Koopmans G, Blokland A, Scheepens A (2004) Learning and adult neurogenesis: survival with or without proliferation? Neurobiol Learn Mem 81:1–11
Rola R, Mizumatsu S, Otsuka S, Morhardt DR, Noble-Haeusslein LJ, Fishman K, Potts MB, Fike JR (2006) Alterations in hippocampal neurogenesis following traumatic brain injury in mice. Exp Neurol 202:189–199
Santarelli L, Saxe M, Gross C et al (2003) Requirement of hippocampal neurogenesis for the behavioral effects of antidepressants. Science 301:805–809
Saxe MD, Battaglia F, Wang JW et al (2006) Ablation of hippocampal neurogenesis impairs contextual fear conditioning and synaptic plasticity in the dentate gyrus. Proc Natl Acad Sci USA 103:17501–17506
Shors TJ, Miesegaes G, Beylin A, Zhao M, Rydel T, Gould E (2001) Neurogenesis in the adult is involved in the formation of trace memories. Nature 410:372–376
Shors TJ, Townsend DA, Zhao M, Kozorovitskiy Y, Gould E (2002) Neurogenesis may relate to some but not all types of hippocampal-dependent learning. Hippocampus 12:578–584
Smart TG, Hosie AM, Miller PS (2004) Zn2+ ions: modulators of excitatory and inhibitory synaptic activity. Neuroscientist 10:432–442
Sokolov EN, Nezlina NI (2004) Long-term memory, neurogenesis, and signal novelty. Neurosci Behav Physiol 34:847–857
Strosznajder R, Gajkowska B (2006) Effect of 3-aminobenzamide on Bcl-2, Bax and AIF localization in hippocampal neurons altered by ischemia-reperfusion injury. The immunocytochemical study. Acta Neurobiol Exp (Wars) 66:15–22
Suh SW, Listiack K, Bell B et al (1999) Detection of pathological zinc accumulation in neurons: methods for autopsy, biopsy, and cultured tissue. J Histochem Cytochem 47:969–972
Takeda A (2000) Movement of zinc and its functional significance in the brain. Brain Res Brain Res Rev 34:137–148
Takeda A (2001) Zinc homeostasis and functions of zinc in the brain. Biometals 14:343–351
Takeda A, Takefuta S, Okada S, Oku N (2000) Relationship between brain zinc and transient learning impairment of adult rats fed zinc-deficient diet. Brain Res 859:352–357
Takeda A, Minami A, Takefuta S, Tochigi M, Oku N (2001) Zinc homeostasis in the brain of adult rats fed zinc-deficient diet. J Neurosci Res 63:447–452
Takeda A, Minami A, Seki Y, Oku N (2003) Inhibitory function of zinc against excitation of hippocampal glutamatergic neurons. Epilepsy Res 57:169–174
Takeda A, Minami A, Seki Y, Oku N (2004) Differential effects of zinc on glutamatergic and GABAergic neurotransmitter systems in the hippocampus. J Neurosci Res 75:225–229
Takeda A, Tamano H, Nagayoshi A, Yamada K, Oku N (2005) Increase in hippocampal cell death after treatment with kainate in zinc deficiency. Neurochem Int 47:539–544
Takeda A, Kanno S, Sakurada N, Ando M, Oku N (2008a) Attenuation of hippocampal mossy fiber long-term potentiation by low micromolar concentrations of zinc. J Neurosci Res 86:2906–2911
Takeda A, Yamada K, Tamano H, Fuke S, Kawamura M, Oku N (2008b) Hippocampal calcium dyshomeostasis and long-term potentiation in 2-week zinc deficiency. Neurochem Int 52: 241–246
Treves A, Rolls ET (1994) Computational analysis of the role of the hippocampus in memory. Hippocampus 4:374–391
van Praag H, Schinder AF, Christie BR, Toni N, Palmer TD, Gage FH (2002) Functional neurogenesis in the adult hippocampus. Nature 415:1030–1034
Wang FD, Zhao FJ, Jing NH (1999) Effect of dietary zinc on microtubule-associated protein 2 expression in the brain of mice. Sheng Li Xue Bao 51:495–500
Wang FD, Bian W, Kong LW, Zhao FJ, Guo JS, Jing NH (2001) Maternal zinc deficiency impairs brain nestin expression in prenatal and postnatal mice. Cell Res 11:135–141
Wang ZY, Danscher G, Dahlstrom A, Li JY (2003) Zinc transporter 3 and zinc ions in the rodent superior cervical ganglion neurons. Neuroscience 120:605–616

Wang X, Wang ZY, Gao HL, Danscher G, Huang L (2006) Localization of ZnT7 and zinc ions in mouse retina—immunohistochemistry and selenium autometallography. Brain Res Bull 71:91–96

Winocur G, Wojtowicz JM, Sekeres M, Snyder JS, Wang S (2006) Inhibition of neurogenesis interferes with hippocampus-dependent memory function. Hippocampus 16:296–304

Zhang L, Chi ZH, Ren H, Rong M, Dahlstrom A, Huang L, Wang ZY (2007) Immunoreactivity of zinc transporter 7 (ZNT7) in mouse dorsal root ganglia. Brain Res Bull 74:278–283

Zhang LH, Wang X, Stoltenberg M, Danscher G, Huang L, Wang ZY (2008) Abundant expression of zinc transporters in the amyloid plaques of Alzheimer's disease brain. Brain Res Bull 77:55–60